

Assessment of the Influence of Weather Conditions and Dust Accumulation on Solar Energy Production of Al-Hussein Bin Talal Power Plant

Rabaa K. Al-Farajat¹, Omar Al-Khashman², Hani M. Alnawafleh^{3*}

¹Department of Mechanical Engineering, Faculty of Engineering, Al-Hussein Bin Talal University, Ma'an, Jordan

²Department of Environmental Engineering, Faculty of Engineering, Al-Hussein Bin Talal University, Ma'an, Jordan

³Department of Mining and Mineral Engineering, Faculty of Engineering, Al-Hussein Bin Talal University, Ma'an, Jordan

Email: rabaafarajat1996@gmail.com, omarkhashman@yahoo.com, *hanialnawafleh@ahu.edu.jo

How to cite this paper: Al-Farajat, R.K., Al-Khashman, O., Alnawafleh, H.M. (2025) Assessment of the Influence of Weather Conditions and Dust Accumulation on Solar Energy Production of Al-Hussein Bin Talal Power Plant. *Journal of Environmental Protection*, 16, 647-667.

<https://doi.org/10.4236/jep.2025.167033>

Received: June 5, 2025

Accepted: July 19, 2025

Published: July 22, 2025

Copyright © 2025 by author(s) and Scientific Research Publishing Inc. This work is licensed under the Creative Commons Attribution International License (CC BY 4.0).

<http://creativecommons.org/licenses/by/4.0/>



Open Access

Abstract

Photovoltaic solar energy is a vital resource in addressing global environmental and climate change challenges, with particular significance in Jordan. However, the weather, which varies with time, has a significant impact on how efficient solar photovoltaic systems are. This study investigates how various weather patterns affect a photovoltaic system's energy output. The effects of several meteorological variables were examined using Multivariate Linear Regression (MLR), and the chemical makeup of the dust settling on the PV panels and in the surrounding area was evaluated. Primary data from a 3.02 MW solar power system at Al-Hussein Bin Talal University (AHU) in Ma'an, Jordan, were gathered at different periods. According to the findings, weather conditions explained 14.9% of the variation in energy output in 2021 but 34.1% in 2022. The most common component in the dust, silica, was found to have relatively modest levels of heavy metals, suggesting that anthropogenic sources were the primary causes of dust pollution.

Keywords

Photovoltaic Solar Energy, Weather Conditions, Dust Accumulation, Al-Hussein Bin Talal University, Data Collection, Power Plant Performance

1. Introduction

Solar power has become a key component in providing access to low-cost and reliable electricity [1]. In fact, the world's installed capacity for solar energy is expand-

ing rapidly to accommodate energy demand. The installed capacity of PV technology increased from 72,236 MW to 1,055,072 MW from 2011 to 2022 [2].

The electrical power generation capacity of a power station will differ according to many factors, like the location of the plant, PV technology itself, the capacity of the plant, and meteorological variables. Also, the productivity of PV plants fluctuates with time, which causes a decline in the reliability of the network because of changes in weather conditions, especially temperature and solar radiation [3]. Ideal operating conditions for PV panels or standard test conditions (STC) are the amount of radiation (1000 W/m^2), temperature (25°C), and sun spectrum 1.5 AM [4]. The best weather conditions for solar power generation are cold, sunny, and windy days. Indeed, the sun powers the panels, the cool air around them keeps them cool, and the cooling effect of the wind on the panels dissipates excess heat generated by the equipment [5]. Because the PV cells are located outdoors, they are exposed to all weather variables such as air temperature, relative humidity, dust, solar radiation, and wind. All of these variables will affect the performance and generation of power from PV cells [6] [7]. For example, by increasing the surface temperature of panels and dust, the power produced by panels will decline [8].

Temperature and the amount of solar radiation are the most critical factors that affect the PV performance and productivity. Variations in atmospheric conditions like temperature and solar radiation during the day have a significant impact on module efficiency. As concluded by Karafil *et al.* [9], the panel voltage slightly increases while panel current grows according to the level of solar radiation. In a similar vein, panel power rises in direct proportion to solar radiation. Conversely, panel temperature causes a proportionate drop in panel voltage and a slight increase in panel current. Since the rate of voltage decline is greater than the rate of current increase, panel power decreases [9]. In fact, the system produces more power throughout the winter with a 71.1% power differential compared to that in the summer. In this case, voltages are greater than summer voltages by 483%. In contrast, the module currents decrease in the winter compared to the summertime current at 46.7% [10]. Furthermore, it was found that for every 1°C increase in solar cell temperature, there was a loss in electrical efficiency of 0.06% and a decrease in output power of roughly 0.37 W. whereas the output power increased by 2.94 W for every 100 W/m^2 increase in amount of radiation, which was in turn accompanied by a 4.93°C rise in solar cell temperature [11].

Wind can directly control the energy produced from PV by influencing the module temperature and dust deposition. In a study conducted in Saudi Arabia, the temperature lowered by up to 10°C with wind speeds between 2.8 - 5.3 m/s, and in Slovenia by half at 12 m/s. Furthermore, the wind can prevent dust deposition by blowing dust particles off the PV module surface [12]. For instance, a study conducted in Egypt demonstrates that wind-driven dust deposition from the module decreases at a specific tilt angle. Nevertheless, it has an adverse effect on the desert region since the wind generates a considerable quantity of dust and sand particles. In Libya, dust accumulates on the PV surface at a great rate and with rapidity be-

cause of air-wind circulation [13].

Burduhos *et al.* [14] clarified that relative humidity has different effects, either negatively or positively, on PV performance. Adverse effects such as high humidity under certain temperature and pressure conditions can cause condensation on the surface of PV modules. Dewdrops reflect incoming solar radiation, so the amount of incoming solar radiation will decline. On the other hand, condensation of vapor at the PV surface leads to a decrease in temperature, thus increasing productivity. Rusănescu *et al.* confirmed that moisture on the PV panels has the potential to alter the behavior of solar radiation, which might affect the open circuit voltage [15].

Comparatively, all suspended atmospheric substances such as sand, dust, pollutants, smoke, dirt, pollen, etc., are expressed in most studies as dust, which acts as a barrier between PV and radiation, reducing total solar radiation that comes from the sun because it covers and corrodes the solar panel [16]. Indeed, dust accumulation affects the efficiency of PV modules more than other weather conditions. On the other hand, all of the weather conditions are hard to avoid as dust accumulates; consequently, dust particles can be removed by natural or artificial cleaning. It was recently announced that anti-soiling coatings can be utilized as an active approach to mitigate the impact of contamination on PV module performance [17] (Güngör *et al.*, 2022). Dust can markedly produce shading effects, thus leading to hot spots on the PV cell, which in turn can increase the temperature of the PV cell and then complicate thermal stress that works on performance degradation and possible cell damage. Additionally, it also has a heat-trapping effect inside the PV cells [18]. Various factors affect dust accumulation, mainly the dust's physical qualities (weight, density, and geometry of the particles), its chemical composition, and the site's ambient and meteorological factors. In fact, fine dust particles generally reduce PV solar cells' efficiency more than coarser ones [19]. More discussion on the impact of weather conditions and dust accumulation on solar energy production is found in Tasie *et al.* [20] and Zarei *et al.* [21].

The Middle East and North Africa (MENA) countries have enormous potential to develop and deploy solar technologies because of the high levels of solar radiation. On the other hand, the region's extreme weather conditions and desert environment create a serious challenge to the progress and development of solar energy production [22]. However, Jordan has a high potential for wind resources, with annual average wind speeds exceeding 7 m/s (altitude of 10 m) in some districts. It also has one of the highest solar radiation potentials in the world at 4 - 8 kWh/m² and more than 300 days of sunshine in the region [23]. For this reason, Jordan is recognized as one of the sunniest regions in the world. Also, because 80% of Jordan's areas are desert regions with little to no cloud cover and rainfall, solar energy is actually a promising renewable energy source that can be used in power generation in Jordan [24]. The installed capacity of solar PV in Jordan is growing rapidly, as shown in **Figure 1**. Indeed, the installed capacity of PV increased from 287 MW in 2016 to 1914 MW in 2022 [2].

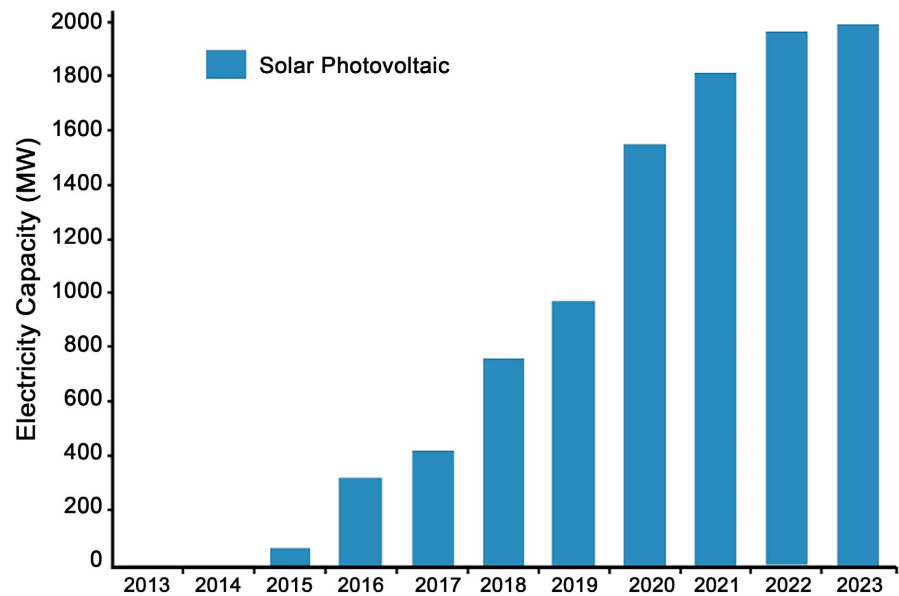


Figure 1. Installed capacity of solar PV in Jordan [2].

Ma'an is a governorate in the south of Jordan, which is located between latitudes 29° to $31^{\circ}30'N$ and $35^{\circ}30'$ to $38^{\circ}E$ longitude and has an area of 33373.4 km^2 which is around 37% of the total area of Jordan [25]. It is categorized as one of the areas with the highest solar direct radiation and low diffuse radiation in Jordan, with broad flatlands appropriate for large-scale PV systems. As a result, many large-scale government-owned projects are being built in this area. It also has a high air density, and wind speeds may reach 12 m/s on some days [26]. On the other hand, in desert areas like Ma'an region, there are several difficulties in terms of the installation and operation of PV systems due to the highly variable weather conditions; temperatures, high wind speeds, and dust density in the surroundings all reduce the efficiency of using PV systems [27]. Ma'an elevation differs from 1630 m above sea level in the southeast to 1104 m in the east, and the average annual temperature is $24^{\circ}C$ [28]. Also, Ma'an summers have a hot and dry climate, while winters are mild to cold. Its annual rainfall is around 50 mm/year. Additionally, the average maximum daylight hours occur in June at a rate of 12.6 h/day, while the average minimum daylight hours in winter (December and January) are about 7.0 h/day [29]. Besides, Ma'an governorate is considered to be an extensive reservoir of mineral and industrial rocks that act as a critical aspect of Jordan's mining industry. Rocks such as sandstone, phosphate, limestone, coquina, dolomite, clay, and various types of aggregates are the particular sources of several industries in the region [28].

Although Ma'an area is attractive for investments in PV projects due to the large solar radiation, it suffers from the problem of dust and its accumulation on the cells, as it is considered one of the most important factors that reduce the performance of the cells. It is the purpose of this paper to assess the influence of weather conditions and dust accumulation on solar energy production of Al-Hussein Bin

Talal Power Plant.

2. Methods and Data Collection

2.1. The Study Area

AL-Hussein Bin Talal solar power plant was selected for this study. It is located in Al Hussein Bin Talal University (AHU) campus within the northwest part of Ma'an governorate. The AHU is located 210 km south of Amman and 150 km northeast of the Aqaba governorate along the desert highway connecting Saudi Arabia and Jordan and covers an area of 11 km². Accordingly, in a deal with a foundation for control systems, AHU agreed to build, run, and transfer ownership of a solar-powered electrical power generation station on campus for ten years. Following that, the university will acquire ownership of the station and all of its production [30]. This plant started to run in 6/2017 with 9600 polycrystalline modules, each with a capacity of 315 W; furthermore, it was built on an area of 5.5 hectares. With a total peak operating capacity of 3.02 MW, the power plant is grid-connected. And the modules are set at a 27° tilt angle, facing south (0° azimuth angle). Cleaning methods are manual cleaning with water, which occurs twice a year. An aerial photo of this plant and the PV array of Sadeen contracting [31] are shown in **Figure 2(a)** and **Figure 2(b)** respectively.

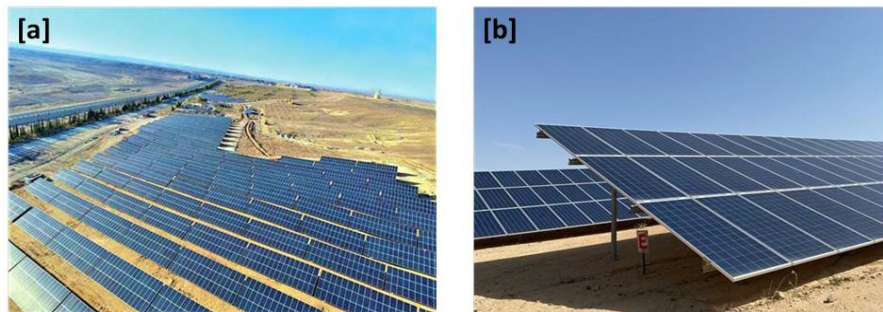


Figure 2. AHU solar power plant (a) An aerial photo of the study area and (b) PV array in the study area.

Polycrystalline modules from Jinko Solar Company were used in the power plant, each with a peak capacity of 315 W. The datasheet for the module used in the power plant, derived at standard test conditions (STC), is clarified in **Table 1**.

2.2. Weather and Productivity Data Collection

Weather and productivity data were collected from more than one source; it was collected from a period extending from 1/2/2021 until 30/9/2021 and from 1/2/2022 until 30/9/2022, as these periods show fluctuations in weather conditions due to the change of seasons. Temperature and amount of radiation data were collected from the power plant, as it contains weather stations that record the ambient weather conditions. Furthermore, it is connected to control and

Table 1. Datasheet of a Solar PV Module at STC.

Maximum power (P_{max})	315 W
Maximum power voltage (V_{mp})	37.2 V
Maximum power current (I_{mp})	8.48 A
Open-circuit voltage (V_{oc})	46.2 V
Short-circuit current (I_{sc})	9.01 A
Module efficiency	16.23%
Number of cells	72
Dimensions	1956*992*40 mm
Temperature coefficients of P_{max}	-0.40%/°C
Temperature coefficients of V_{oc}	-0.30%/°C
Temperature coefficients of I_{sc}	0.06%/°C
Fill factor	75.6%
NOCT	45°C

monitoring systems that are inside the command-and-control room contained in the station. **Figure 3** illustrates the weather station inside the power plant, which is mounted on an expandable tripod. It contains pyranometers, temperature and relative humidity sensors, wind speed sensors, and wind direction sensors. This equipment, as shown in a figure, can be powered by a solar power system. **Figure 4** shows weather data on the monitoring and productivity systems screen. System productivity data during the same period was also collected from the power plant itself by existing records through existing control (monitoring) and productivity systems records inside the power plant.

**Figure 3.** Weather station inside the power plant.



Figure 4. Weather data at the control and productivity systems screen.

On the other hand, relative humidity, wind speed, and wind direction data weren't obtained from the same station. As meteorological stations provide only the monthly average, data on relative humidity, wind speed, and direction were collected from NASA for surface meteorology and solar energy.

The quality control steps for data collection are: 1) All of the energy meters and weather stations (such as temperature, sun radiation, and wind speed) have been verified and regularly calibrated under the manufacturer's specifications. 2) The weather data obtained has been compared with records from registered weather stations to ensure accuracy and consistency. 3) The process of documenting the times of periodic maintenance of equipment or its replacement operations, in addition to documenting the times of washing the panels, ensures reliable data collection.

2.3. Accumulated Dust Samples: Collection & Analyses

Using a fine brush, accumulated dust on the PV cell's surface at the power plant was collected to know the chemical composition of the dust and its effect on raising the cell temperature. Dust samples were taken in two different periods, the first during the wet season in the month of March 2023, while the other sample was collected during the dry season in July 2023. The collected dust samples were analyzed experimentally for their chemical composition using the X-ray fluorescence (XRF)-EDX 7000 available at the laboratories of engineering faculty at Al-Hussein Bin Talal University. **Figure 5** shows accumulated dust on a PV surface.



Figure 5. Accumulated dust on a PV surface.

To identify the statistics of chemical elements in the dust of the study area, ten samples of settled dust were collected during the dry season (August 2022). The settled dust particles were collected in polyethylene containers (dimension: 30 cm in diameter and 15 cm deep) installed on 60 cm tripods for two months located on the roofs of high buildings (3 - 4 m above the ground) to eliminate the effect of soil or debris from plants. The samples of dust were weighted and converted to mg/m³/day. The dust samples were sieved and particles < 50 μm size to remove any particles or debris materials and dried in an oven at 105°C. A flame atomic absorption spectrophotometer (Shimadzu AAS model AA-6200, Japan) was used to analyze heavy metals in the standard metal solutions (Merck Company, Germany) alongside the soil sample solutions. All the standard solutions were prepared from analytical-grade compounds from Merck Company. The calibration curve was prepared for each of the metals investigated using least-squares fitting. By analyzing a reference standard material (SRM) from soil 7 from the International Atomic Energy Agency (IAEA), the accuracy of this procedure has been assessed. The accuracy is better than ±5%, according to the SRM study. The accuracy of the results was assessed through repeat analysis (three replicates for each sample). During the experimental analysis, all glassware was Pyrex washed several times with soap, distilled water, and diluted nitric acid to remove any adhered impurities [32] [33].

2.4. Data Analysis

2.4.1. Weather Data Analysis

A PV module's maximum power output (P_{max}) under local weather conditions can be calculated by:

$$P_{max} = P_{max-STC} \times [1 + \beta \times (T - T_{STC})] * \frac{G}{G_{STC}} \quad (1)$$

where β is temperature coefficient of P_{max} , and G is the amount of radiation.

Fill factor (FF), which is the ratio of actual maximum power to I_{sc} and V_{oc} and can be calculated by:

$$FF = \frac{P_{max}}{I_{sc} \times V_{oc}} \quad (2)$$

The power output can be greater when the FF is better. I_{sc} is proportional to G , while V_{oc} is proportional to module temperature (T_{PV}). The actual I_{sc} and V_{oc} in the field are given by:

$$I_{sc} = I_{sc-STC} \times G \quad (3)$$

$$V_{oc} = V_{oc-STC} - \alpha \times \text{number of cells} \times (T_{PV} - 25) \quad (4)$$

where α is the temperature coefficient of V_{oc} . I_{sc} and V_{oc} values are explained in **Table 1**, T_{PV} is a module temperature that can be calculated by:

$$T_{PV} = T_a + \frac{(NOCT - 20)}{800} \times G \quad (5)$$

where T_a is the ambient temperature, NOCT is a nominal operating cell tempera-

ture [34]. The term “ambient temperature” refers to the temperature of the embracing environment, typically the air temperature. Furthermore, relative humidity (RH) is the actual amount of water vapor in the air as a percentage of the total amount of vapor that can exist in the air at its current temperature [7].

2.4.2. Multivariate Linear Regression

In order to identify the coefficients of effect for each weather condition (temperature, radiation, wind speed, and relative humidity) on the produced energy for 2021 and 2022, MLR was used. Produced energy is the quantity of energy that was generated; it is commonly expressed in megawatt-hours (MWh) or kilowatt-hours (kWh), depending on the size of production and consumption [35]. Regression analysis is a popular method for analyzing multifactor data. It involves creating a suitable mathematical equation that connects a group of predictor variables (independent variables) with the response variable (*i.e.*, dependent variable). The ability of the MLR model to examine the connection between multiple independent variables and multiple dependent variables at the same time led to its choice. When the dataset contains several variables that will probably influence various correlated outcomes, this method of analysis works particularly effectively, as it enhances descriptive effectiveness and power by considering the interrelated relationships between several dependent variables.

In this work, the daily system-produced energy is regarded as the response variable, while each weather condition is considered a predictor variable. Consequently, the MLR model equation proposed in this work takes the following forms in 2021 and 2022, respectively:

$$\text{produced}_{\text{energy } 2021} = 18.373 - 0.088x_1 + 0.006x_2 - 0.31x_3 - 0.188x_4 \quad (6)$$

$$\text{produced}_{\text{energy } 2022} = 8.474 - 0.017x_1 + 0.012x_2 - 0.011x_3 - 0.173x_4 \quad (7)$$

where x_1 is ambient temperature, x_2 radiation, x_3 relative humidity, and x_4 wind speed. This equation was arrived at through the following:

In order to be able to apply the regression analysis test, we ensure that the data is normally distributed, as shown in **Figure 6(a)** and **Figure 6(b)**. The extent to which the variables follow a normal distribution is shown in **Figure 7(a)** and **Figure 7(b)**.

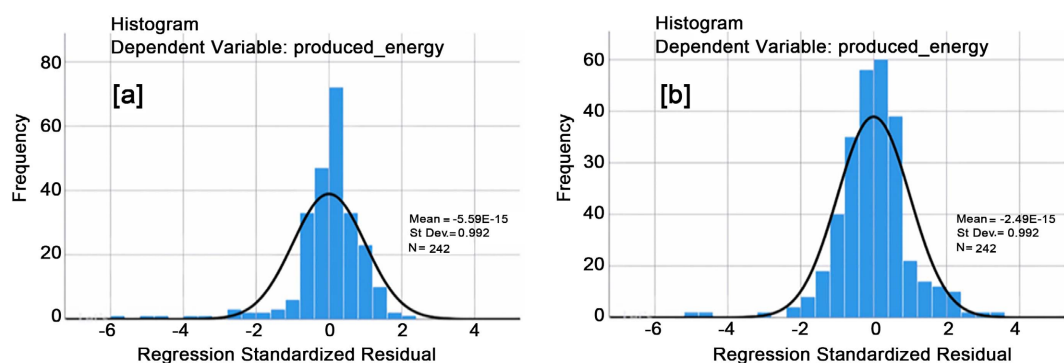


Figure 6. Histograms of standardized regression (a) in 2021 and (b) in 2022.

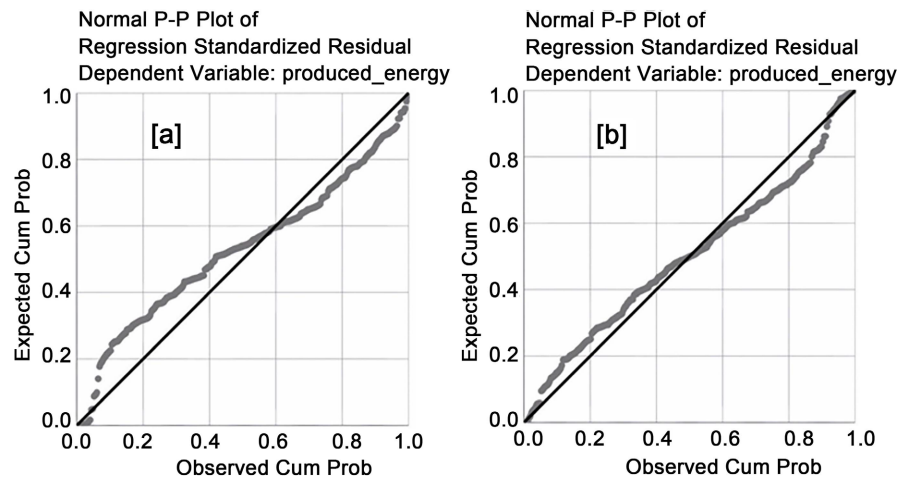


Figure 7. The extent to which the variables follow a normal distribution (a) in 2021 and (b) in 2022.

Furthermore, **Figure 8(a)** and **Figure 8(b)** show the scatter line, which indicates that the linearity condition for applying the variance test is met.

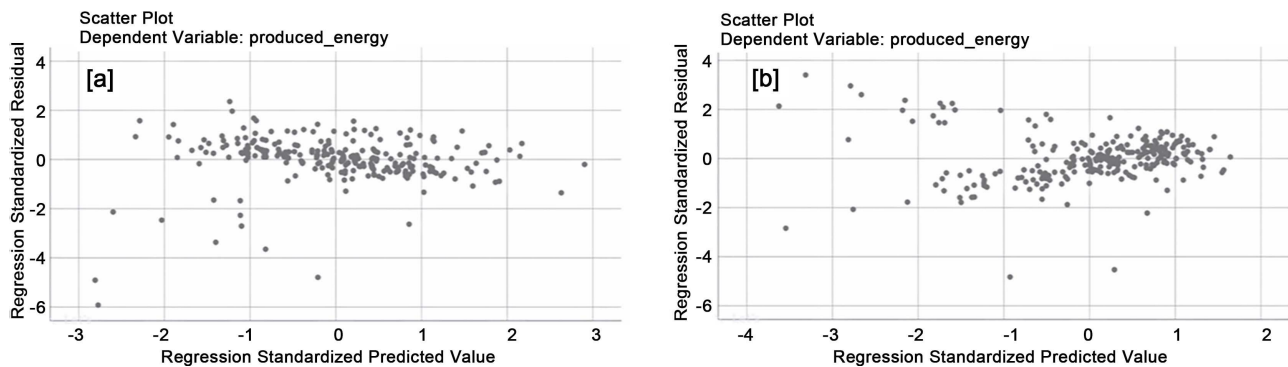


Figure 8. Scatterplot for (a) 2021 and (b) 2022.

2.4.3. Wind Rose

A wind rose is a graphical representation utilized by meteorologists to concisely display how the wind blows. Furthermore, wind speed and direction are usually distributed over a specific area. The bar plot wind rose shows the probability of time the wind blows in particular speed ranges by separating each section of the plot into distinct colors [36]. There are several ways to draw a wind rose. WRPLOT View is a fully functional wind rose program for weather data. Provides visual wind rose charts, frequency analysis, and charts for multiple weather data formats.

3. Results and Discussion

3.1. Chemical Composition of Dust Particles at PV Surface

The chemical composition results (**Table 2**) suggest several dust particles sources, mainly rock crushers due to quarries abundant in Ma'an governorate. These dust

particles have a direct effect on light absorption, scattering, transmission, and reflection. This, in turn, affects the amount of solar radiation that reaches the PV surface. It is evident that the dust accumulated on the surface of PV modules in the study area is mainly rich in Calcium Oxide (CaO), Silicon Dioxide (SiO₂), and Aluminum Oxide (Al₂O₃) with different percentages. It also contains other compounds but in smaller proportions. In the wet season, the dust sample was rich with 39.453% CaO generated mainly from limestone. Followed by 38.692% of SiO₂, which comes primarily from quartz-rich sandstone. While in the dry season, SiO₂ content reached 48.364%, followed by 23.225% CaO.

Additionally, the collected dust samples were rich in components of carbon-based soot, red soil with oxidized iron, and limestone, which are the three common air pollutants with high light absorption coefficients. Moreover, SiO₂ which is considered a non-metallic particle had a higher percentage than Fe₂O₃ which is considered a metallic particle. Thus, the percentage of absorbed light from the particles is lower because of the ability of metallic particles to absorb light at a faster rate than non-metallic particles. Furthermore, due to the desert nature of the study area, the shape of dust particles is mainly angular and irregular, thus in turn leaving the PV panels with a rough surface, which increases the risk of adhesion and makes dust removal more difficult. All of these facts are reported by Almkhhtar *et al.* [18]. The types of dust that settle on solar PV differ based on their geographical location. The elements that could be present are mainly from exhaust gases, organic and inorganic particles containing soluble and insoluble salts, and due to road traffic which generates zinc, manganese, and lead. Cadmium, Sulphur, and antimony from car brake shoe wear. Fossil fuel burning can also produce dust [15].

Table 2. Result of the chemical composition quantities of the dust sample at the PV surface.

Chemical compound	Quantitative result % in wet season	Quantitative result % in dry season
CaO	39.453%	23.225%
SiO ₂	38.692%	48.364%
Al ₂ O ₃	8.605%	14.359%
Fe ₂ O ₃	5.610%	6.635%
MgO	3.563%	3.747%
TiO ₂	1.337%	1.374%
K ₂ O	1.332%	1.768%
SO ₃	0.467%	0.035%
P ₂ O ₅	0.260%	0.151%
Tm ₂ O ₃	0.129%	0.000%
Cl	0.126%	0.000%
ZrO ₂	0.115%	0.092%
SrO	0.107%	0.063%

Continued

MnO	0.094%	0.116%
V ₂ O ₅	0.048%	0.000%
ZnO	0.032%	0.019%
Cr ₂ O ₃	0.022%	0.017%
PbO	0.005%	0.003%
Ir ₂ O ₃	0.004%	0.005%
CuO	0.000%	0.018%
Rb ₂ O	0.000%	0.008%

3.2. Metal Concentration in Dust Samples for the Study Area

The analytical results of the level of metals in the dust samples were summarized in **Table 3**. Based on the results of the analysis for the metals (Cu, Fe, Cd, Pb, Zn, Cr, and Ni), observed that metals originating from anthropogenic activities were distributed in dust samples by atmospheric deposition within a distance depending on the grain size of the dust particles, direction and strength of the wind, the type of soil, and major physico-chemical parameters such as pH, electrical conductivity (EC), and cation exchange capacity (CEC) of the soil. The lead value in the dust samples ranged from 981 to 1431 ppm, with a mean value of 1240 ppm. The highest value of a lead, 1431 ppm, was measured in the dust samples collected from the eastern side of the entrance and the northeastern area of the study area. However, the lower lead concentration 981 ppm was measured in the samples collected west of the studied area (reference sample) 2 km west of the studied area. The high lead level in dust samples beside the investigated area can be attributed to anthropogenic activities such as burning fossil fuels and heavy traffic activity in and around the studied area [29] [37]-[40].

Iron is one of the principal metals in the Earth's crust and is mainly associated with other sources; it's generally deposited in the neighborhood of the emission sources [37] [41] [42]. Higher values of iron were measured on the eastern side of the studied area (13,950 ppm), but the lowest value of iron (8902 ppm) was found in the dust sample where the sample was collected around 50 m away from the entrance to the university, beside the parking site. However, the higher value of iron was also found in the nearby mechanical vehicles and traffic sites outside the university camp. In general, cadmium was found to be lower in concentration compared to the other metals in dust. The mean concentration of Hg in the dust was 143 ppm, while the range of Hg in samples varied from 61 to 232 ppm. The high value of zinc in dust samples was associated mainly with the emission sources of human activities and traffic emissions in the area studied. The highest copper concentration was measured near the vegetation areas in the east and northwest of the studied area. This result shows that the sources of contamination, such as anthropogenic activities, agricultural soils receive metals mainly from fertilizers, pesticides, manure, and other scattered diffuse pollution sources such as traffic emis-

sions and incineration [37] [43] [44].

Table 3. Statistical of all chemical elements in dust samples in ppm.

Elements	Max	Min	Mean	Standard deviation
Si	57,560	31,112	34,105	7231
Ca	48,255	35,170	44,118	2991.4
Ba	2816	1182	2181	718.5
Fe	33,860	22,101	24,181	40723
Mn	6624	5280	5680	622.4
Ni	240	103	192	60.4
Cu	2840	1312	1820	431.4
Zn	1560	1287	1430	109.7
Pb	1431	981	1240	150.7
Hg	232	61	143	65.2
S	17,200	8240	11,800	2988.4
Cl	9700	4827	5687	4321.2

3.3. Analysis of Weather Conditions

3.3.1. Comparison of Energy Production

The weather data averages during 2021 and 2022 are shown in **Table 4**. These summarize monthly temperature, solar radiation, wind speed, relative humidity, and average energy produced, in addition to average electrical characteristics for 2021 and 2022, respectively. These data show the temperature in 2022 decreased by a 2.5% drop compared to 2021. In contrast, in 2022 compared to 2021, the proportion of solar radiation increased by 19.3%, relative humidity climbed by 0.98%, and wind speed fell by 0.57%. Where the percentage of energy produced was reduced between 2022 and 2021 by -0.18%, as determined by:

$$\text{reduction in produced energy} = \frac{\text{produced energy in 2022} - \text{produced energy in 2021}}{\text{produced energy in 2021}} \times 100 \quad (8)$$

Table 4. Average monthly I_{sc} , T_c , V_{oc} , produced energy, and weather conditions.

		I_{sc} (A)	T_c (°C)	V_{oc} (V)	Produced energy (MWh)	Radiation (W/m ²)	T_a (°C)	Wind speed (m/s)	Relative humidity (%)
2021	February	4.21	28.17	45.68	15.8	465.4	13.6	4.18	62.3
	March	5.34	35.31	44.54	18.5	592.8	16.8	4.6	54.9
	April	4.88	38.5	44.03	18	542.6	21.5	4.2	38.3
	May	5.65	56.26	41.17	17.3	627.9	36.7	4.6	28.2
	June	5.68	53.4	41.64	17.2	631.4	33.6	4.7	34.4
	July	6	51.54	41.93	16.9	666.6	30.7	4.9	34.9

Continued

2022	August	6.09	51.94	41.87	16.6	676.3	30.8	4.3	33.4
	September	6.19	57.51	40.97	16.9	687.4	36	4.18	43.3
	February	4.71	38.71	43.99	15.7	523.4	22.3	3.9	66.8
	March	7.16	49.83	42.21	17.55	794.7	25	4.5	59.9
	April	6.98	48.53	42.42	17.52	775.6	24.3	4.4	28.5
	May	7.06	49.32	42.29	17.93	783.9	24.8	4.8	30.5
	June	6.64	52.17	41.83	16.8	737.2	29.13	4.6	35.3
	July	6.99	53.44	41.63	18	776.9	29.16	4.7	35.5
	August	6.62	54.78	41.41	17.6	735.3	31.8	4.4	33.9
	September	6.37	50.5	42.1	16	707.5	28.3	4	42.6

3.3.2. Multivariate Linear Regression Models Result

The coefficients of effect for each weather condition on the energy produced by the power plant were evaluated using MLR. **Table 5** shows the statistics for 2021 and 2022 of each factor affecting energy production in 2021 and 2022 respectively.

Table 5. Descriptive statistics for 2021 and 2022.

	2021			2022		
	Mean	Std. Deviation	N	Mean	Std. Deviation	N
Produced energy	17.210	2.159	242	17.1778	2.212	242
T_amb	27.610	9.131	242	25.3360	6.863	242
Radiation	613.030	139.105	242	731.7562	114.548	242
Relative humidity	41.037	14.697	242	41.4398	16.433	242
wind speed	4.490	1.236	242	4.464	1.299	242

Moreover, **Table 6** shows the strength of the correlation between independent variables and the dependent variable, as the correlation value was 0.387 for 2021 and 0.584 for 2022, which represents a good value. The coefficient of determination (R^2) was 0.149 in 2021 and 0.341 in 2022, indicating that the independent variables explained 14.9% of the variance in the dependent variable in 2021 and 34.1% in 2022. R^2 values suggest that only a small percentage of the variations in PV production can be explained by the model. This indicates that the weather variables chosen for the study weren't the only ones that influenced the impact on PV system performance. Some unmeasured variables influence PV output, for instance: Over time and panel degradation lower efficiency, potential issues, inverter efficiency, shading from the surrounding plants, mismatch losses, additional electrical inefficiencies or wiring losses, and cloud cover.

Table 7 shows the significance and suitability of the regression model for use. The value of F for both years, with a significance of 0.00 (smaller than 0.05) indicates the suitability of the model for use.

Table 6. Correlation strength in 2021 and 2022.

	Model	R	R Square	Adjusted R Square	Std. Error of the Estimate
2021	1	0.387 ^a	0.149	0.135	2.008
2022	1	0.584 ^a	0.341	0.330	1.811

a. Predictors: (Constant), wind speed, relative, radiation, T_{amb} ; b. Dependent Variable: produced energy.

Table 7. Significance and suitability of the regression model for use in 2021 and 2022.

ANOVA ^a							
	Model		Sum of Squares	df	Mean Square	F	Sig.
2021	1	Regression	167.881	4	41.970	10.406	0.000 ^b
		Residual	955.857	237	4.033		
		Total	1123.737	241			
2022	1	Regression	401.712	4	100.428	30.609	0.000 ^b
		Residual	777.603	237	3.281		
		Total	1179.315	241			

a. Dependent Variable: produced energy; b. Predictors: (Constant), wind speed, radiation, relative humidity, T_{amb} .

Most importantly, the independent variables that had the most influence on the dependent variable are shown in **Table 8**. For 2021, the lowest significant value was 0.00 in favor of the variables (T_{amb} , radiation), and the impact relationship (Equation (6)) is given. For 2022, as all of them had a significant effect and the variance between them was very small, but the most influential of them on the dependent variable, which is 0.001, was in favor of the variable (radiation), followed by a moral value of 0.01 for the variable (relative humidity), and finally a moral value of 0.02 in favor of the variable (T_{amb}) and thus, the impact relationship (Equation (7)) is given. The size of effect (Eta squared) of each independent variable on produced energy in 2021 and 2022 is shown in **Table 9**.

3.3.3. Wind Rose Analysis

Wind has a big role in affecting the working and productivity of solar cells as it helps in cooling the PV panels and can positively or negatively impact solar cell dust removal or addition. **Figure 9** displays the wind rose diagram for a period extending from the 1st of February until the 30th of September for both years. The wind rose diagram indicates that the prevailing wind direction in the study area is between North-North-West (NNW) and West-North-West (WNW) in both

Table 8. Coefficients of weather variables in 2021 and 2022.

Model	Coefficients ^a					Correlations			
	Unstandardized Coefficients		Standardized Coefficients	t	Sig.	Zero-order	Partial	Part	
	B	Std. Error	Beta						
2021 1	(Constant)	18.373	1.165		15.766	0.000			
	T_amb	-0.088	0.021	-0.374	-4.219	0.000	-0.082	-0.264	-0.253
	radiation	0.006	0.001	0.358	5.509	0.000	0.270	0.337	0.330
	Relative humidity	-0.031	0.012	-0.212	-2.512	0.013	-0.044	-0.161	-0.150
	wind speed	-0.188	0.105	-0.108	-1.796	0.074	-0.117	-0.116	-0.108
2022 1	(Constant)	8.474	1.411		6.006	0.000			
	T_amb	0.017	0.022	0.053	0.771	0.441			
	radiation	0.012	0.001	0.607	10.611	0.000			
	relative	0.011	0.010	0.084	1.172	0.242			
	wind speed	-0.173	0.091	-0.102	-1.913	0.057			

a. Dependent Variable: produced energy.

Table 9. Eta squared for independent variables in 2021 and 2022.

	2021		2022	
	Eta	Eta Squared	Eta	Eta Squared
produced energy * T_amb	0.798	0.637	0.635	0.403
produced energy * radiation	0.949	0.901	0.841	0.706
produced energy * relative	0.994	0.987	0.942	0.888
produced energy * wind speed	0.955	0.911	0.908	0.824

years. From wind class frequency distribution (Figure 10), wind speed was varying and the highest wind speed reached 10 m/s on one of the days of 2021, whereas, the highest measured wind speed during 2022 was about 8.8 m/s.

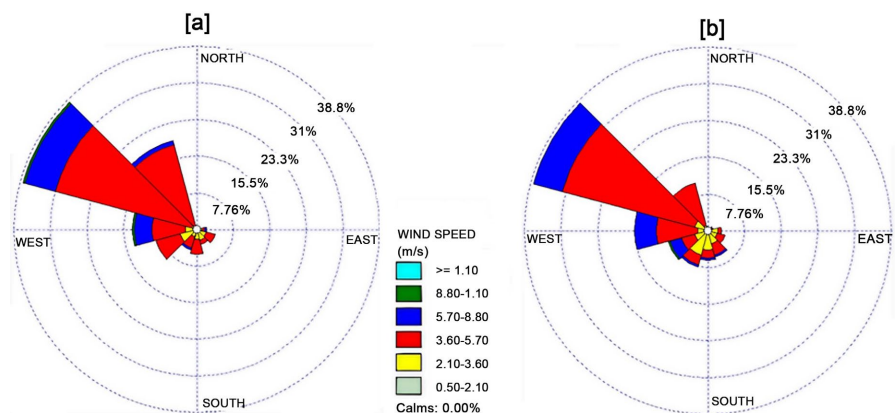


Figure 9. Wind rose for the study area in 2021 and 2022.

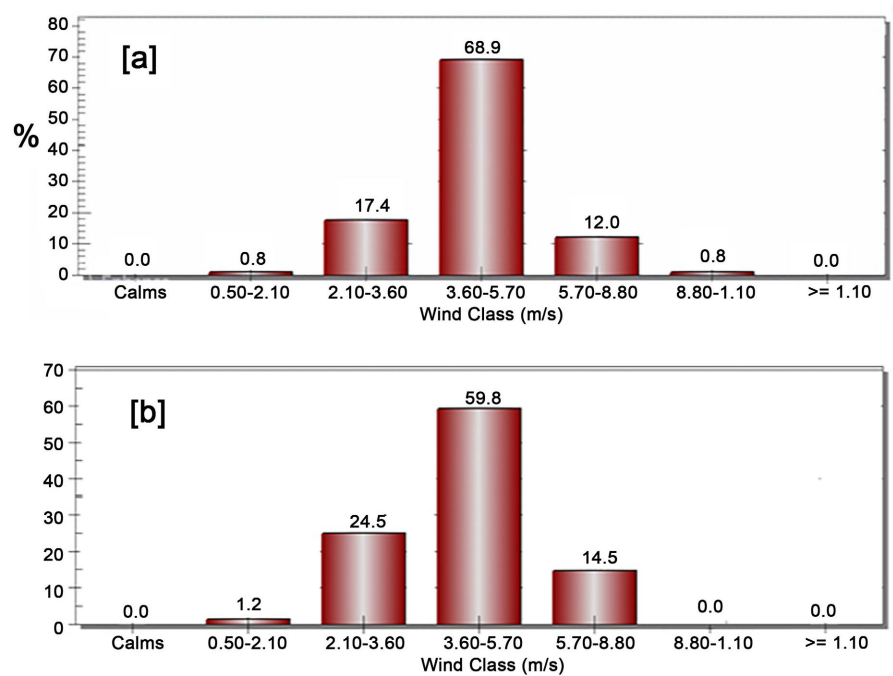


Figure 10. Wind class frequency distribution for 2021 and 2022.

4. Conclusions

1) The dust that covers the surface of PV in the wet season is mainly composed of 39.453% CaO, followed by 38.692% SiO₂. While in the dry season, SiO₂ content reached 48.364%, followed by 23.225% CaO; both also contain other compounds, but in smaller proportions. The source of these chemical composition quantities is mainly limestone and quartz-rich sandstone.

2) The analytical results showed that the lead value ranged from 981 ppm to 1431 ppm, while the Si value ranged from 31,112 - 57,560 ppm, with a larger percentage inside the sample, after evaluating the dust samples for the research region. On the other hand, iron levels ranged from 13,950 ppm to 8902 ppm. It was frequently discovered that cadmium concentrations in dust were lower than those of the other metals. The samples' Hg concentrations varied from 61 to 232 ppm. Based on these data, it can be concluded that the primary causes of contamination are human activities like burning fossil fuels and heavy traffic in and around the area under study.

3) The research area's predominant wind directions are West-North-West (WNW) and North-North-West (NNW). Additionally, wind speed varied.

4) The temperature in 2022 decreased by 2.5%. On the other hand, the percentage of solar radiation in 2022 increased by 19.3%, while relative humidity increased by 0.98% in 2022 and wind speed decreased by 0.57% in 2022, all compared to 2021 and the percentage of the reduction in produced energy was equal to -0.18% between 2021 and 2022.

5) In 2022, the correlation coefficient (R^2) between the independent variables and the dependent variable was 0.341, indicating that 34.1% of the variance in the

dependent variable could be explained by the independent variables. In comparison, the R^2 value in 2021 was 0.149, showing that only 14.9% of the variance was explained, suggesting an improvement in explanatory power over the year.

5. Recommendations

1) Because the plant is situated near a crucial route and in a desert region, it is strongly advised to raise the frequency of PV surface cleaning to more than twice a year.

2) As a barrier to lowering the percentage of dust surrounding the power plant, it is advised to work to increase the amount of plant cover in the region.

3) This study suggests ongoing research on the same power plant against hard environmental elements as well as extreme weather circumstances.

4) It is advised to enhance PV panels' resistance to weather, particularly in arid regions, by adding features like self-cleaning technology and anti-soiling coating.

Authors' Contributions

All authors contributed to collecting data, data analysis, interpretation of data and writing this article and approved the article. Rabaa Al-Farajat: collection of sampling, analysis of sampling, literature review, writing-original draft; Omar Ali Al-Khashman: data curation, writing-original draft; data interpretation and visualization, final approval of the manuscript: literature review and editing; Hani Al-nawafleh: writing-review and editing, data interpretation and visualization, and formatting the final manuscript and approval of the manuscript.

Conflicts of Interest

The authors declare no conflicts of interest regarding the publication of this paper.

References

- [1] Maka, A.O.M. and Alabid, J.M. (2022) Solar Energy Technology and Its Roles in Sustainable Development. *Clean Energy*, **6**, 476-483. <https://doi.org/10.1093/ce/zkac023>
- [2] International Renewable Energy Agency (IRENA) (2022) Solar Energy. <https://www.irena.org/Energy-Transition/Technology/Solar-energy>
- [3] Al-Waeli, A.H.A., Sopian, K., Kazem, H.A. and Chaichan, M.T. (2017) Photovoltaic/Thermal (PV/T) Systems: Status and Future Prospects. *Renewable and Sustainable Energy Reviews*, **77**, 109-130. <https://doi.org/10.1016/j.rser.2017.03.126>
- [4] Dash, P.K., Gupta, N.C., Rawat, R. and Pant, P.C. (2017) A Novel Climate Classification Criterion Based on the Performance of Solar Photovoltaic Technologies. *Solar Energy*, **144**, 392-398. <https://doi.org/10.1016/j.solener.2017.01.046>
- [5] Doddy Clarke, E. and Sweeney, C. (2022) Solar Energy and Weather. *Weather*, **77**, 90-91. <https://doi.org/10.1002/wea.4124>
- [6] Perraki, V. and Kounavis, P. (2016) Effect of Temperature and Radiation on the Parameters of Photovoltaic Modules. *Journal of Renewable and Sustainable Energy*, **8**, Article 013102. <https://doi.org/10.1063/1.4939561>

- [7] Hamdi, R.T., Hafad, S.A., Kazem, H.A. and Chaichan, M.T. (2018) Humidity Impact on Photovoltaic Cells Performance: A Review. *International Journal of Recent Engineering Research and Development*, **3**, 27-37. <http://www.ijrerd.com/papers/v3-i11/5-IJRERD-C264.pdf>
- [8] Owhaib, W., Borett, A., AlKhalidi, A., Al-Kouz, W. and Hader, M. (2022) Design of a Solar PV Plant for Ma'an, Jordan. *IOP Conference Series: Earth and Environmental Science*, **1008**, Article 012012. <https://doi.org/10.1088/1755-1315/1008/1/012012>
- [9] Karafil, A., Ozbay, H. and Kesler, M. (2016) Temperature and Solar Radiation Effects on Photovoltaic Panel Power. *Journal of New Results in Science*, **5**, 48-58. <https://dergipark.org.tr/en/pub/jnrs/issue/27333/287728>
- [10] Chaichan, M.T. and Kazem, H.A. (2016) Experimental Analysis of Solar Intensity on Photovoltaic in Hot and Humid Weather Conditions. *International Journal of Scientific & Engineering Research*, **7**, 91-96. <https://www.uotechnology.edu.iq/paper/PDF/power/No.%202020.pdf>
- [11] Rahman, M.M., Hasanuzzaman, M. and Rahim, N.A. (2015) Effects of Various Parameters on PV-Module Power and Efficiency. *Energy Conversion and Management*, **103**, 348-358. <https://doi.org/10.1016/j.enconman.2015.06.067>
- [12] Shaik, F., Lingala, S.S. and Veeraboina, P. (2023) Effect of Various Parameters on the Performance of Solar PV Power Plant: A Review and the Experimental Study. *Sustainable Energy Research*, **10**, Article No. 6. <https://doi.org/10.1186/s40807-023-00076-x>
- [13] Hasan, K., Yousuf, S.B., Tushar, M.S.H.K., Das, B.K., Das, P. and Islam, M.S. (2021) Effects of Different Environmental and Operational Factors on the PV Performance: A Comprehensive Review. *Energy Science & Engineering*, **10**, 656-675. <https://doi.org/10.1002/ese3.1043>
- [14] Burduhos, B.G., Visa, I., Duta, A. and Neagoe, M. (2018) Analysis of the Conversion Efficiency of Five Types of Photovoltaic Modules during High Relative Humidity Time Periods. *IEEE Journal of Photovoltaics*, **8**, 1716-1724. <https://doi.org/10.1109/jphotov.2018.2861720>
- [15] Rusănescu, C.O., Rusănescu, M., Istrate, I.A., Constantin, G.A. and Begea, M. (2023) The Effect of Dust Deposition on the Performance of Photovoltaic Panels. *Energies*, **16**, Article 6794. <https://doi.org/10.3390/en16196794>
- [16] Kazem, H.A., Chaichan, M.T., Al-Waeli, A.H.A. and Sopian, K. (2020) A Review of Dust Accumulation and Cleaning Methods for Solar Photovoltaic Systems. *Journal of Cleaner Production*, **276**, Article 123187. <https://doi.org/10.1016/j.jclepro.2020.123187>
- [17] GÜNGÖR, O., Kahveci, H. and Gökçe, H.S. (2023) The Effect of Various Industrial Dust Particles on the Performance of Photovoltaic Panels in Turkey. *Environmental Science and Pollution Research*, **30**, 15128-15144. <https://doi.org/10.1007/s11356-022-23216-0>
- [18] Almukhtar, H., Lie, T.T., Al-Shohani, W.A.M., Anderson, T. and Al-Tameemi, Z. (2023) Comprehensive Review of Dust Properties and Their Influence on Photovoltaic Systems: Electrical, Optical, Thermal Models and Experimentation Techniques. *Energies*, **16**, Article 3401. <https://doi.org/10.3390/en16083401>
- [19] Marashli, A., Al Shaba'an, G.N., Al-Twaissi, W., Shalby, M. and Al-Rawashdeh, H. (2022) Impact of Accumulated Dust on Performance of Two Types of Photovoltaic Cells: Evidence from the South of Jordan. *International Journal of Renewable Energy Development*, **11**, 547-557. <https://doi.org/10.14710/ijred.2022.42625>
- [20] Tasie, N.N., Sigalo, F.B., Omubo-Pepple, V.B. and Israel-Cookey, C. (2022) Model-

- ling of Solar Power Production in Dry and Rainy Seasons Using Some Selected Meteorological Parameters. *Energy and Power Engineering*, **14**, 274-290. <https://doi.org/10.4236/epe.2022.147015>
- [21] Zarei, T., Abdolzadeh, M. and Yaghoubi, M. (2022) Comparing the Impact of Climate on Dust Accumulation and Power Generation of PV Modules: A Comprehensive Review. *Energy for Sustainable Development*, **66**, 238-270. <https://doi.org/10.1016/j.esd.2021.12.005>
- [22] Javed, W., Guo, B., Wubulikasimu, Y. and Figgis, B.W. (2016) Photovoltaic Performance Degradation Due to Soiling and Characterization of the Accumulated Dust. 2016 *IEEE International Conference on Power and Renewable Energy (ICPRE)*, Shanghai, 21-23 October 2016, 580-584. <https://doi.org/10.1109/icpre.2016.7871142>
- [23] Shalby, M., Abuseif, A., Gomaa, M., Salah, A., Marashli, A. and Al-Rawashdeh, H. (2022) Assessment of Dust Properties in Ma'an Wind Farms in Southern Jordan. *Jordan Journal of Mechanical and Industrial Engineering*, **16**, 645-652.
- [24] Akash, O.B., Abu Abdo, A.M., Mohsen, M.S. and Akash, B.A. (2016) A Note on Solar Energy Research in Jordan. *International Journal of Applied Engineering Research*, **11**, 7100-7105. <https://www.ripublication.com/Volume/ijaerv11n10.htm>
- [25] AL-Taani, A., Al-husban, Y. and Farhan, I. (2021) Land Suitability Evaluation for Agricultural Use Using GIS and Remote Sensing Techniques: The Case Study of Ma'an Governorate, Jordan. *The Egyptian Journal of Remote Sensing and Space Science*, **24**, 109-117. <https://doi.org/10.1016/j.ejrs.2020.01.001>
- [26] Abdalla, M. and Abuquba, H. (2019) Natural Cooling of Two Axis Tracking Photovoltaic Module. *Energy Sources, Part A: Recovery, Utilization, and Environmental Effects*, **45**, 2436-2452. <https://doi.org/10.1080/15567036.2019.1663300>
- [27] AL-Sawalmeh, W.H., Alrashdan, M.H.S. and Alashaa'ry, H.A.M. (2021) Experimental Monitoring System Using Arduino Microcontroller in Studying the Effect of Temperature and Light Intensity of Solar Cell Output Power in Ma'an Development Area. *International Journal of Smart Grid and Clean Energy*, **10**, 157-161. <https://doi.org/10.12720/sgce.10.2.157-161>
- [28] Tarawneh, K. (2019) The Geology, Stratigraphy and Structure of Ma'an Area, South Jordan. *Journal of Environment and Earth Science*, **9**, 103-117.
- [29] Al-Khashman, O.A. (2013) Assessment of Heavy Metals Contamination in Deposited Street Dusts in Different Urbanized Areas in the City of Ma'an, Jordan. *Environmental Earth Sciences*, **70**, 2603-2612. <https://doi.org/10.1007/s12665-013-2310-6>
- [30] Arabia Weather (2016) An Agreement to Invest Solar Energy at Al-Hussein Bin Talal University. <https://www.arabiaweather.com/en/content/an-agreement-to-invest-solar-energy-at-alhussein-bin-talal-university>
- [31] Sadeen Contracting. https://sadeencontracting.com/?thegem_pf_item=solar-plant-al-hussein-bin-talal-university
- [32] Alsbou, E.M.E. and Al-Khashman, O.A. (2018) Heavy Metal Concentrations in Roadside Soil and Street Dust from Petra Region, Jordan. *Environmental Monitoring and Assessment*, **190**, Article 48.
- [33] Jaradat, Q.M. and Momani, K.A. (1999) Contamination of Roadside Soil, Plants, and Air with Heavy Metals in Jordan, A Comparative Study. *Turkish Journal of Chemistry*, **23**, 209-220. <https://journals.tubitak.gov.tr/chem/vol23/iss2/13>
- [34] Alrwashdeh, S.S. (2018) Assessment of Photovoltaic Energy Production at Different

- Locations in Jordan. *International Journal of Renewable Energy Research*, **8**, 797-804.
- [35] Jaber, J., Marahleh, G. and Dalabeeh, A. (2019) Emissions Reduction Resulting from Renewable Energy Projects in Jordan. *Journal of Energy Technologies and Policy*, **9**, 42-51.
- [36] Roubeyrie, L. and Celles, S. (2018) Windrose: A Python Matplotlib, Numpy Library to Manage Wind and Pollution Data, Draw Windrose. *Journal of Open Source Software*, **3**, Article 268. <https://doi.org/10.21105/joss.00268>
- [37] Carreras, H.A. and Pignata, M.L. (2002) Biomonitoring of Heavy Metals and Air Quality in Cordoba City, Argentina, Using Transplanted Lichens. *Environmental Pollution*, **117**, 77-87. [https://doi.org/10.1016/s0269-7491\(01\)00164-6](https://doi.org/10.1016/s0269-7491(01)00164-6)
- [38] Tüzen, M. (2003) Determination of Heavy Metals in Soil, Mushroom and Plant Samples by Atomic Absorption Spectrometry. *Microchemical Journal*, **74**, 289-297. [https://doi.org/10.1016/s0026-265x\(03\)00035-3](https://doi.org/10.1016/s0026-265x(03)00035-3)
- [39] Banat, K.M., Howari, F.M. and Al-Hamad, A.A. (2005) Heavy Metals in Urban Soils of Central Jordan: Should We Worry about Their Environmental Risks? *Environmental Research*, **97**, 258-273. <https://doi.org/10.1016/j.envres.2004.07.002>
- [40] Han, Y.M., Du, P.X., Cao, J.J. and Posmentier, E.S. (2006) Multivariate Analysis of Heavy Metal Contamination in Urban Dusts of Xi'an, Central China. *Science of the Total Environment*, **355**, 176-186. <https://doi.org/10.1016/j.scitotenv.2005.02.026>
- [41] Berg, T., Røyset, O., Steinnes, E. and Vadset, M. (1995) Atmospheric Trace Element Deposition: Principal Component Analysis of ICP-MS Data from Moss Samples. *Environmental Pollution*, **88**, 67-77. [https://doi.org/10.1016/0269-7491\(95\)91049-q](https://doi.org/10.1016/0269-7491(95)91049-q)
- [42] Al-Khashman, O.A. and Shawabkeh, R.A. (2009) Metal Distribution in Urban Soil around Steel Industry beside Queen Alia Airport, Jordan. *Environmental Geochemistry and Health*, **31**, 717-726. <https://doi.org/10.1007/s10653-009-9250-9>
- [43] Wong, M.H., Wong, J.W.C. and Chen, T.B. (1996) Trace Metal Contamination of the Hong Kong Soil Environment: A Review. In: *Contaminants and the Soil Environment in the Australasia-Pacific Region*, Springer, 501-511. https://doi.org/10.1007/978-94-009-1626-5_16
- [44] Biasioli, M., Barberis, R. and Ajmone-Marsan, F. (2006) The Influence of a Large City on Some Soil Properties and Metals Content. *Science of the Total Environment*, **356**, 154-164. <https://doi.org/10.1016/j.scitotenv.2005.04.033>